Mar Biodiv (2011) 41:365–382
DOI 10.1007/s12526-010-0067-7

SENCKENBERG

''MARINE BIODIVERSITY UNDER CHANGE''

Seasonal and diel vertical migration of zooplankton in the High Arctic during the autumn midnight sun of 2008

Ananda Rabindranath · Malin Daase · Stig Falk-Petersen · Anette Wold · Margaret I. Wallace · Jørgen Berge · Andrew S. Brierley

Received: 30 April 2010 / Revised: 6 October 2010 / Accepted: 25 October 2010 / Published online: 30 November 2010

Abstract The diel vertical migration (DVM) of *Calanus* (*Calanus finmarchicus*, *Calanus glacialis* and *Calanus hyperboreus*) and *Metridia longa* was investigated in August 2008 at six locations to the north and northwest of Svalbard (Rijpfjorden, Ice, Marginal Ice Zone, Shelf break, Shelf and Kongsfjorden). Despite midnight sun conditions, a diel light cycle was clearly observed at all stations. We collected data on zooplankton vertical distribution using a Multi Plankton Sampler (200-μm mesh size) and an EK60 echosounder system (38, 120 and 200 kHz). These were supplemented by environmental data collected using a standard conductivity, temperature and depth (CTD) profiler. The sea ice had recently opened in Rijpfjorden, Ice and Shelf stations, and these stations exhibited phytoplankton bloom conditions with pronounced fluorescence maxima at approximately 30 m. In contrast, Kongsfjorden was more representative of autumn conditions, with the Arctic bloom having culminated 2–3 months prior to sampling. All three *Calanus* species were found shallower than 50 m on average at Rijpfjorden and the Ice station, while *C. glacialis* and *C. hyperboreus* were found deeper than 200 m on average at Kongsfjorden. Shallow water DVM behaviour (<50 m) was observed at Rijpfjorden and the Shelf station, especially among the *C. finmarchicus* CI-CIII population, which was particularly abundant at the Shelf (>5,000 individuals/m^3). A bimodal depth distribution was observed among *C. finmarchicus* at the Shelf break station, with CI-CIII copepodites dominating at depths shallower than 100 m and CIV-adult stages dominating at depths exceeding 600 m. Statistical analyses revealed significant differences between the day and night 200-kHz data, particularly at specified depth strata (25–50 m) where backscatter intensity was higher during the day, especially in Rijpfjorden and at the Ice station. We conclude that DVM signals exist in the Arctic during late summer/autumn, when a need to feed and an abundant food source exists, and these signals are primarily due to mesozooplankton.

Keywords Arctic Ocean · Diel vertical migration · *Calanus* · Phytoplankton bloom · Seasonal vertical migration

This article belongs to the special issue ''Marine Biodiversity under Change''

A. Rabindranath (✉) · A. S. Brierley
Pelagic Ecology Research Group, Scottish Oceans Institute,
The University of St Andrews,
St Andrews, Fife KY16 8LB, UK
e-mail: aar8@st-andrews.ac.uk

M. Daase · S. Falk-Petersen · A. Wold
Norwegian Polar Institute,
Polarmiljøsenteret,
9296, Tromsø, Norway

J. Berge
The University of Norway in Svalbard,
9171, Longyearbyen, Svalbard, Norway

M. I. Wallace
The British Oceanographic Data Centre,
Proudman Oceanographic Laboratory,
Liverpool, UK

S. Falk-Petersen
Department of Arctic and Marine Biology, Faculty of Biosciences,
Fisheries and Economics, University of Tromsø,
9037, Tromsø, Norway

Introduction

Copepods of the genus *Calanus* are the dominant herbivores in Arctic seas in terms of species biomass, and play a key role in pelagic food webs (Kwasniewski et al. 2003).

Three species of *Calanus* coexist (the *Calanus* complex) in the Svalbard region and together make up 50–80% of the total mesozooplankton biomass (Søreide et al. 2008). *C. hyperboreus* is a High Arctic oceanic species, *C. glacialis* is associated with Arctic shelf waters, and *C. finmarchicus* dominates in Atlantic waters (Daase and Eiane 2007; Daase et al. 2007; Blachowiak-Samolyk et al. 2008). All these copepods are rich in lipids and represent an important food source for other zooplankton and many pelagic fish species (Falk-Petersen et al. 1990; Kwasniewski et al. 2003).

The depth distribution of *Calanus* in colder regions is characterised by strong seasonality and linked closely to the annual cycle of primary production (Vinogradov 1997). Copepods are found in shallow waters during the productive summer months and in deeper waters during winter (Varpe et al. 2007). The widely accepted paradigm of polar marine biology is that the seasonal changes in sea-ice cover have a dramatic influence on ecosystem processes (Cisewski et al. 2009; Søreide et al. 2010; Leu et al. 2010). For much of the year in seasonally ice covered areas such as the high Arctic, most of the primary production occurs in the overlying sea-ice and not in the water column (Arrigo and Thomas 2004), and ice cover is known to have a significant negative effect on phytoplankton primary production in the Arctic (Gosselin et al. 1997). However, as the sea-ice melts, phytoplankton production peaks in summer and autumn, and is accompanied by peak abundances of *Calanus* close to the surface (Smith and Sakshaug 1990; Falk-Petersen et al. 2008, 2009). The phytoplankton bloom follows the receding ice edge as it melts during spring/summer (Zenkevitch 1963; Sakshaug and Slagstad 1991), and the onset of the Arctic phytoplankton bloom varies widely in the Svalbard region due to large differences in prevailing sea-ice conditions (Søreide et al. 2008).

Along the western coast of Svalbard, where the influence of ice is diminished by the dominance of warmer Atlantic Water (>3°C), the phytoplankton bloom starts in April/May (Leu et al. 2006). In contrast, the phytoplankton bloom in northern and eastern Svalbard is strongly influenced by the reduction in light levels beneath sea-ice cover, and the bloom onset may be delayed until the sea-ice thins sufficiently to permit illumination, which may occur as late as August (Falk-Petersen et al. 2000; Hegseth and Sundfjord 2008). When primary production decreases following the phytoplankton bloom, copepods descend to depth and overwinter in a state of dormancy (Heath et al. 2004), during which time they survive on large lipid reserves accumulated during the summer (Conover and Huntley 1991; Hagen and Auel 2001). Whether *Calanus* ascend later in areas with heavier sea-ice cover due to a delay in the Arctic bloom is largely unknown, although Falk-Petersen et al. (2009) and Søreide et al. (2010) suggest that the seasonal ascent of *Calanus glacialis* is timed with the Arctic bloom, and that ice algae may be as important as phytoplankton in terms of a food source for copepods in ice covered seas (Søreide et al. 2006). Hunt et al. (2002) suggest that in ice covered waters, an early ice retreat in late winter (when there is insufficient light to support a bloom) will delay the phytoplankton bloom until late spring when the water column is stratified sufficiently to prevent the algae sinking. In contrast, a later ice retreat in spring (when there is sufficient light to support a bloom), allows an earlier ice-associated bloom to develop in "ice-melt-stabilised" water (Hunt et al. 2002).

Whilst populations migrate on a large scale seasonally, individuals also migrate on a daily basis. The vertical migration of copepods is considered to be an effective strategy for coping with variations in food availability and predation risk throughout the water column (Longhurst 1976). As fish search for their prey visually (Yoshida et al. 2004), *Calanus* have evolved a predator avoidance behaviour known as diel vertical migration (DVM) (Hays 2003). This daily migration is characterised by the en masse ascent of zooplankton populations into food rich surface waters during darkness, followed by a retreat to depth during the day in an attempt to effectively avoid visual predation.

DVM is considered less important at high latitudes than seasonal migration patterns (Kosobokova 1978; Longhurst et al. 1984; Falkenhaug et al. 1997). Previous studies of zooplankton in Arctic regions have largely failed to demonstrate any coordinated vertical migration during the period of midnight sun, when there is little variability in insolation throughout the diel cycle (Blachowiak-Samolyk et al. 2006). Co-ordinated vertical migrations tend to resume towards autumn when a more marked diel cycle develops (Fischer and Visbeck 1993). The conventional paradigm is that DVM behaviour ceases completely during the winter period in the High Arctic due to low food availability in the water column (Smetacek and Nicol 2005) and the over-wintering strategies of the copepods (Falk-Petersen et al. 2008).

In recent years, a variety of instruments and techniques have been used to discover two modes of vertical migration in the high Arctic. Cottier et al. (2006) used an Acoustic Doppler Current Profiler (ADCP) to measure the net vertical velocities of zooplankton during both the Arctic summer and the Arctic autumn. Although co-ordinated zooplankton vertical migration appeared to be absent during the period of midnight sun, there was strong evidence of unsynchronised vertical migrations of individual animals. Falk-Petersen et al. (2008) took advantage of a record northward position of the Arctic polar ice edge in 2004 to study zooplankton diel and seasonal migration in waters that were usually inaccessible due to ice cover. Using a combination of echosounders and nets, they observed varying migration patterns between the different

copepod species at different locations. These seasonal migration patterns were linked to the timing of the Arctic phytoplankton bloom, while DVM could be explained by the daily light cycle.

A better understanding of zooplankton vertical migration throughout the annual cycle is of critical importance in the context of carbon flux in the oceans. Diel migrants ingest organic material in near-surface waters and produce faecal pellets at depth (Cisewski et al. 2009). This process has the potential to contribute considerably to the vertical transport of carbon and nutrients (Longhurst et al. 1990; Longhurst and Williams 1992; Wexels et al. 2002; Sampei et al. 2004). Disruption of zooplankton vertical migration in the Arctic by ice melt, for example, will thus have important consequences.

The aim of this study was to integrate net sampling and acoustic measurements at a number of locations reflecting a variety of Arctic environments from early to post bloom, and observe copepod seasonal and diel migration patterns. Depth stratified net sampling was used to identify the migrants, while simultaneous calibrated multi-frequency acoustic sampling using a hull mounted EK60 echosounder permitted identification of migration patterns at a high temporal and vertical resolution. Six stations across a large spatial area north and west of the Svalbard Archipelago were sampled, enabling the observation of various intensities of the High Arctic bloom. This permitted the assessment of zooplankton vertical migration behaviour in the context of the influences of different water masses (i.e. Atlantic and Arctic dominated locations) and variability in the intensity of primary productivity.

Materials and methods

Sampling location

The study was undertaken during the period of midnight sun, 2–20 Aug 2008, aboard the ice strengthened British Antarctic Survey (National Environment Research Council) research vessel RRS *James Clark Ross* (Cruise JR210). Samples were collected at six stations around Svalbard (Fig. 1, Table 1).

The marine habitat surrounding the Svalbard archipelago is mainly influenced by Atlantic, Arctic, locally produced and glacial water masses. Atlantic Water (AtW) originates in the warm Gulf Stream, and is characterised by salinities >34.9 and temperatures >3°C (Piechura et al. 2001). The majority of northward flowing AtW is transported to the Svalbard archipelago by the West Spitsbergen Current (WSC). The Arctic water (ArW) found around Svalbard originates in the polar basin, and is carried mainly by the East Spitsbergen Current (ESC) and the South Cape Current (SC), both of which flow across the shelf. ArW maintains a salinity of 34.3–34.8 and temperatures <1°C. AtW regularly mixes with ArW as the water from the WSC is advected on to shelf regions (Svendsen et al. 2002; Willis et al. 2006). Locally-produced and glacial water masses mainly influence the fjords, coastal areas and the shelf of the Svalbard archipelago. In spring and summer, ice-melting results in the formation of cold and fresh melt water (MW), while during autumn and winter cold and saline surface water (SW) is produced during sea-ice formation (Walkusz et al. 2003).

Kongsfjorden opens onto the West Spitsbergen Shelf (WSS), and is heavily influenced by the convergence and mixing of AtW carried northward in the WSC and Arctic

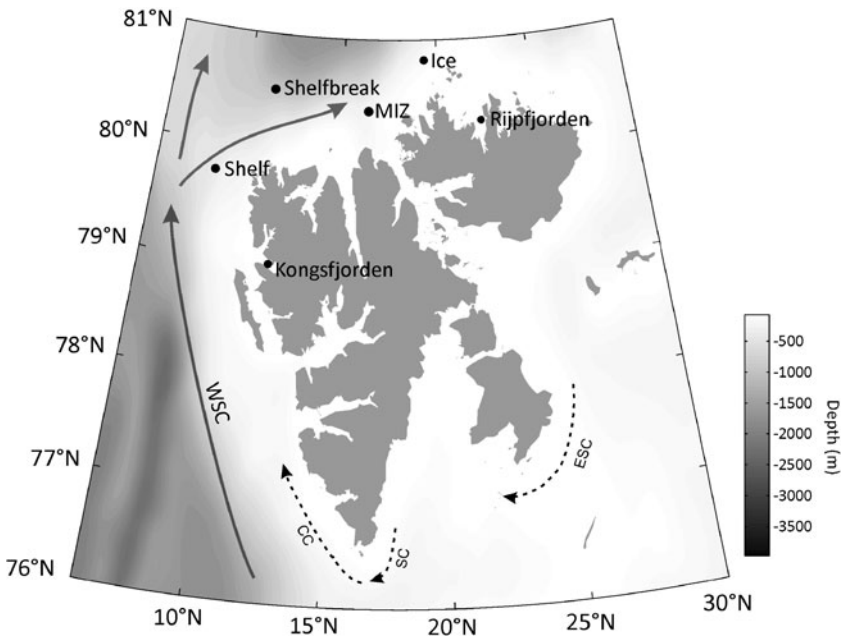

Fig. 1 Sampling station locations and current systems north and west of Svalbard. *Solid arrows* indicate warm water currents, *dotted arrows* cold water currents. *ESC* East Spitsbergen Current, *SC* South Cape Current, *CC* Coastal Current, *WSC* West Spitsbergen Current (see Sampling location for details)

Table 1 Sampling station details including start date and time, station location and maximum water depth

Station	Start date	Start time (UTC)	Latitude (N)	Longitude (E)	Depth (m)	MPS depth strata	MPS sampling time (day; night)
Rijpfjorden (RF)	14/08/2008	20:58	80.285	22.304	225	210-175, 175-100, 100-50, 50-20, 20-0	09:30; 20:45
Ice (ICE)	06/08/2008	09:14	80.812	19.218	138	100-50, 50-20, 20-0	14:00; 23:00
Marginal Ice Zone (MIZ)	08/08/2008	21:43	80.347	16.269	386	375-200, 200-100, 100-50, 50-20, 20-0	12:00; 22:00
Shelf break (SHB)	12/08/2008	08:45	80.487	11.307	753	740-600, 600-200, 200-100, 100-50, 50-0	16:30; 22:30
Shelf (SH)	02/08/2008	14:19	79.725	8.833	449	370-200, 200-100, 100-50, 50-20, 20-0	15:00; 23:00
Kongsfjorden (KF)	18/08/2008	17:58	78.960	11.890	345	320-200, 200-100, 100-50, 50-20, 20-0	06:00; 21:00

and glacial waters (Svendsen et al. 2002; Basedow et al. 2004; Willis et al. 2006). Rijpfjorden in contrast, is less well studied, but is known to be more strongly influenced by ArW (Søreide et al. 2010) and, as a seasonally ice covered fjord, can be subject to high influxes of meltwater (Falk-Petersen et al. 2008).

Environmental parameters

The positions of the sea-ice edge were extracted from sea-ice maps produced by the Norwegian Polar Institute (NPI) (Fig. 2). Photosynthetically active radiation (PAR, 400–700 nm) was measured at the surface at all stations (Fig. 3) using a cosine-corrected flat-head sensor (Quantum Li-190 SA, LiCor, USA). Salinity, temperature, depth and fluorescence were measured by a Seabird conductivity-temperature-depth (CTD) profiler and processed following standard Sea Bird Electronics (SBE) data processing procedures by the Scottish Association for Marine Science (SAMS). CTD profiles measuring temperature, salinity and fluorescence were undertaken immediately prior to all zooplankton sampling events.

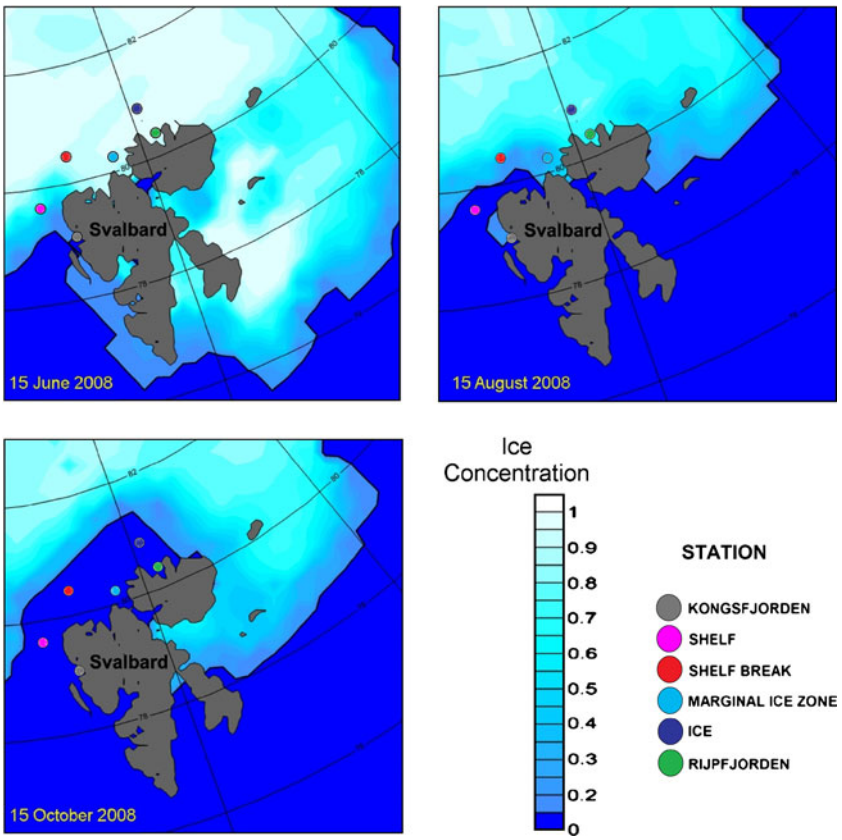

Fig. 2 Ice maps from the Svalbard region courtesy of the Norwegian Polar Institute (NPI) between 15 June and 15 October 2008

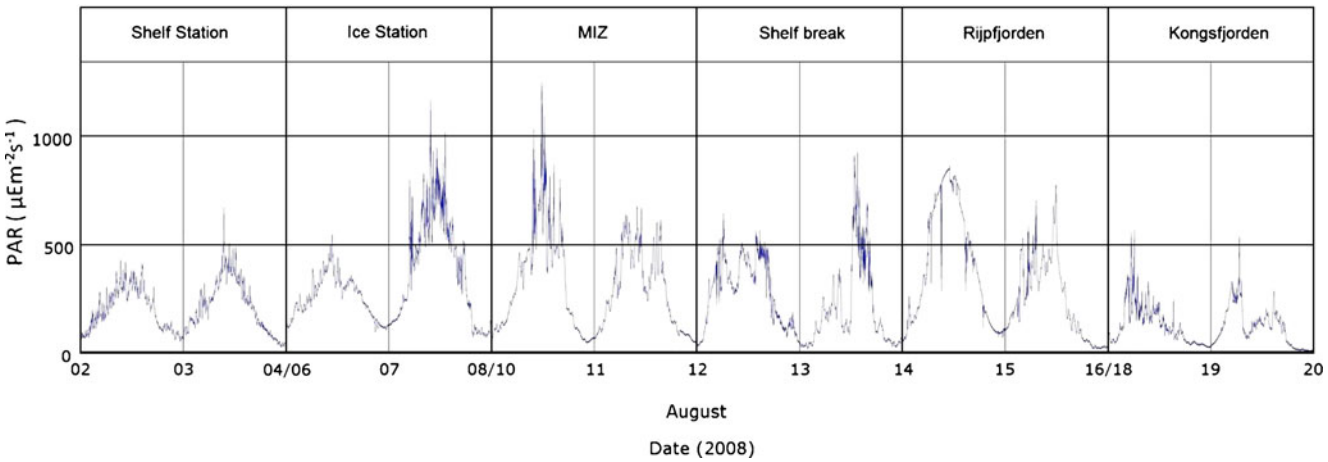

Fig. 3 Surface PAR sampled from the vessel deck at all stations. Stations run in chronological order starting on 02 August 2008 (SH) and ending at 20 August 2008 (KF)

Zooplankton sampling

Mesozooplankton samples were collected at each station as close to local midday and midnight as possible using a Multi Plankton Sampler (MPS, Hydrobios, Kiel) equipped with five nets (200-µm mesh size, 0.25-m^2 opening) that were closed in sequence at discrete depths (detailed in Table 1). The depths of each sequential net were chosen at each station in order to allow comparable surface (i.e. 0–100 m) resolution, while still sampling the entire water column. This procedure was undertaken twice for each sampling event. Filtered water volume was calculated using deployed wire length and the net mouth dimensions, assuming 100% filtration efficiency.

All samples were fixed in 4% formaldehyde and analysed for species composition post cruise. Sorting and identification of the zooplankton were carried out as per Falk-Petersen et al. (1999). *Calanus* species were distinguished on the basis of prosome length (Unstad and Tande 1991; Kwasniewski et al. 2003) and staged from C1-adult. *Calanus* biomass was determined from the collected net abundance data by calculating an average dry weight (DW) value using a collection of published methods (Mumm 1991; Hirche 1991; Richter 1994; Hirche 1997) and published species-specific mass-length relationships (Karnovsky et al. 2003).

Acoustic measurements

A hull mounted Simrad EK60 downward facing echosounder operating at frequencies of 38, 120 and 200 kHz and a ping rate of 0.5 ping s^{-1} was used to gather backscatter information from the water column (6 m depth to near sea bed). At all stations, the ship remained stationary for approximately 24 h while EK60 data were collected, thereby spanning the midday and midnight net sampling regimes. Data were logged using Echolog 60 (SonarData). Use of the ships bowthrusters (which was necessary while the ship was in sea-ice) produced noise spikes and bubble occlusions in the acoustic record. Periods with evident bowthruster-related interference were marked as "bad" and excluded.

The echosounder was calibrated at all frequencies at the end of the cruise, and time varied gain (TVG) amplified noise was removed (Watkins and Brierley 1996). Only data from the upper 125 m of the water column were used due to range limitations, and the near field at 38 kHz (11.90 m) was also excluded from analysis.

We sought to compare data from net samples collected at midday and midnight with acoustic sample data. In order to do this, acoustic data were chosen from each 24-h station to match the zooplankton net sampling times as closely as possible. Whenever possible, 2 h of acoustic data were used to calculate a mean volume backscattering strength {MVBS=10 log10[mean (S_v)]}, and in no cases was less than 1 h of data used. ΔMVBS partitions were carried out using a 1-m×60-ping grid (Benoit et al. 2008) over the entire acoustic sampling period in order to partition the data as follows.

To classify the backscatter, ΔMVBS was calculated (Madureira et al. 1993) using:

$$\Delta\text{MVBS (dB)} = \text{MVBS (dB)}120\text{ kHz} - \text{MVBS (dB)}38\text{ kHz} \quad (1)$$

Mesozooplankton were defined by a ΔMVBS of >12 dB, macrozooplankton/micronekton (including euphausiids) by a ΔMVBS of 2–12 dB, and nekton (including fish and squid) by a ΔMVBS of <2 dB (Madureira et al. 1993). ΔMVBS values were used to partition 200-kHz data from equivalent cells into these three classes, with 200-kHz

mesozooplankton, macrozooplankton, and nekton backscatter now available at each station. The 200-kHz value was chosen at it returns proportionally stronger backscatter from the small *Calanus* zooplankton targeted in this study. Echo integration was then carried out for each taxon using a 25-m × 20–min grid. Nautical area scattering coefficient {NASC = scaled area scattering $[4\pi(1{,}852)^2 s_a]$} values were extracted from the echo integration grids (25 m × 20 min), as these provide linear representations of zooplankton backscatter, which are more easily transformed and analysed using statistical methods.

Although ΔMVBS differentiations were carried out using a 60-ping×1–m depth grid to generate accurate backscatter partitions, the echo integration resolutions were made coarser (25 m×20 min). This coarser resolution was chosen after inspection of the acoustic data revealed that any DVM signal would be of low amplitude and easily "masked" amongst a large number of echo integrations over a very fine scale

Multivariate analysis

Similarity matrices created in PRIMER v 6.19 (Clarke and Gorley 2006) were used to test for differences between the stations based on (1) hydrography, (2) *Calanus* community composition, and (3) zooplankton vertical distributions. Methods employed for each analysis are detailed below.

1. Ten-metre averages of temperature, salinity and fluorescence were calculated over the upper 150 m at each station and then normalised (ranges converted to numerical values with a mean average of zero and standard deviation of 1) in order to summarise the hydrographic conditions. These data were then compared using a Euclidean distance similarity matrix and presented using a hierarchical cluster dendrogram (Fig. 4).
2. Fourth-root transformed MPS determined zooplankton abundances were compared between stations using a Bray-Curtis similarity matrix. Fourth root transformation was chosen to most effectively reduce the significance of differences between large abundances and increase the importance of differences between rare species/stages as suggested by a Draftsman plot of the abundance data. The differences between day and night depth stratified communities, and also between different depth strata at each station were quantified using analysis of similarity (ANOSIM). Negative *R* values for this test indicate greater similarities between groups than within groups, and thus positive *R* values indicate differences between the samples analysed. ANOSIM also generates a significance value for *R* (*p*). Similarity percentage (SIMPER) analysis was carried out to determine which species were most responsible for the observed differences in community structure between day and night samples and different depths in terms of percentage contribution.
3. The partitioned 200-kHz backscatter (mesozooplankton/macrozooplankton/nekton) data were standardised using a 4th-root transformation (in order to analyse the acoustic data in the same form as the zooplankton abundance data) and compared between stations using a Bray-Curtis similarity matrix. The differences between day and night samples and between stations were quantified using ANOSIM and displayed using a multidimensional scaling plot (MDS; Fig. 8). With this plot, the distances between points represent their similarity to each other based on backscatter, with closer points being more similar. The mesozooplankton, macrozooplankton and nekton were also analysed individually between stations to highlight any differences between the different taxa (Fig. 9).

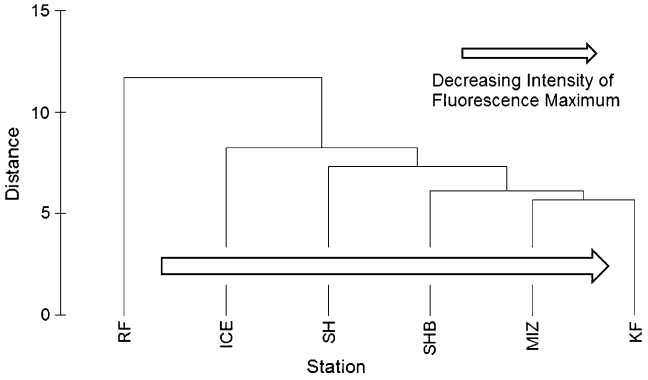

Fig. 4 Dendrogram displaying the Euclidean distance grouping between normalised (ranges converted to numerical values with a mean average of zero and standard deviation of 1) CTD data (10-m averages of temperature, salinity and fluorescence calculated over the top 150 m at each station) at each of the six stations

In order to distinguish between advection and vertical migration effects within the *Calanus* community, the net-determined depth stratified abundances were modified and compared. Firstly, the abundances of all three *Calanus* copepods and *Metridia longa* were summed together at each depth stratum, yielding one value for each depth that represented all the copepods combined. This maintained the depth stratification of the data, but lost all community diversity. The transformed abundance data by this first method shall be referred to subsequently as the depth stratified total abundance. Differences between the day and night samples using this method can be attributed primarily to changing numbers of copepods at each depth stratum. These changes are likely to be good indicators of vertical migration amongst the copepod populations.

Secondly, in order to compare vertical migration effects with possible advection effects, the abundances of each stage of *Calanus* and *Metridia longa* were integrated over the entire water column at each station, resulting in one value for each copepod stage that represented the entire water column depth. This maintained the community diversity within the data, but lost the depth stratification. The transformed abundance data by this second method shall be referred to as the water column community diversity. Differences between the day and night samples using this method will not be a result of changes in vertical position, but rather changing numbers of individuals at the station. This method can be used to assess the advection of copepods in or out of the population.

ANOVA analysis

The partitioned 200-kHz backscatter (mesozooplankton/macrozooplankton/nekton) data were also compared using ANOVA statistical analyses. Firstly, the partitioned backscatter was separated into five depth strata (0–25 m, 25–50 m, 50–75 m, 75–100 m, and 100–125 m). Each depth stratum was then analysed using a three way ANOVA test, with station, taxa and time being the three factors tested for significance. Secondly, all depth strata were combined and the backscatter was analysed using a four-way ANOVA test—with station, taxa, time, and depth now the four factors tested for significance. This allowed the influence of the four primary variables to be ranked and tested for significance.

Results

Ice cover

In June 2008 (prior to our study), most of the Svalbard coast had landfast ice. This ice cover continued around the southern tip of Svalbard and only parts of the west coast were ice-free. However, by the time of our study (August 2008), most of this ice cover had broken up and Kongsfjorden (KF) and the Shelf station (SH) were ice-free. In contrast, the Marginal Ice Zone (MIZ) and Shelf break (SHB) stations were sampled in areas of large leads and broken ice cover, whilst in Rijpfjorden (RF) the fast ice broke up the day before sampling. Ice concentration at the northernmost station, Ice Station (ICE, Fig. 2), was 0.95 at the time of sampling. Continued sea-ice melting and breakup led to large areas north of Svalbard being ice-free by October 2008.

Environmental conditions

Although this study occurred during the period of midnight sun in the High Arctic, a diurnal PAR cycle was observed at all stations (Fig. 3), with daily insolation ranges of 1.2–1,243 $\mu Em^{-2}s^{-1}$. Variability between successive days at the same sampling location was also observed: for example, ICE day 1 (06 Aug) experienced a range of 92.9–543.5 $\mu Em^{-2}s^{-1}$, while ICE day 2 (07 Aug) experienced a range of 70.4–1,159.8 $\mu Em^{-2}s^{-1}$.

Relatively fresh (salinity of 32–33) and cold (−2 to 0°C) water was found over approximately the upper 10 m at ICE, MIZ, SHB, and RF (Fig. 5). However, at MIZ and SHB, water temperatures of 4–4.5°C and higher salinities of around 34–35 were observed between 25 and 30 m depth. Temperatures at RF never exceeded 0°C, while ICE reached approximately 1°C at approximately 100-m depth. A pronounced fluorescence maximum was observed at all four of these ice-influenced stations, corresponding to the boundary between surface MW and deeper AtW/ArW. The precise depth of this fluorescence maximum differed between the ice-influenced stations, but all were found between 20 and 40 m depth. The maximum was most pronounced at ICE and RF, which experienced the most recent sea-ice cover.

SH was dominated by AtW, with temperatures in excess of 6°C and salinities as high as approximately 35 at the surface. A pronounced fluorescence maximum was observed here too. KF was ice-free all year. Although glacial MW influences the fjord, temperatures and salinities indicated AtW dominance. The fluorescence maximum at this station was less pronounced than at the other stations, and this location also experienced only minor changes in light intensity during the diel light cycle compared with the rest of the study area (Figs. 3, 5).

Cluster analysis comparing the stations in terms of temperature, salinity and fluorescence resulted in RF and KF being most extreme in terms of their physical characteristics and the other stations falling between them (Fig. 4).

Copepod populations and vertical distribution

At RF and ICE, young stages (CI-CIII) of *C. finmarchicus* and *C. glacialis* dominated the upper 50 m (>70% of total 0–50 m abundance). *C. hyperboreus* was primarily found as CIV copepodites between 20 to 50 m depth (2.7–7.1 ind m).$^{-3}$ *M. longa* was found in comparatively low abundances ($\leq$2.6 ind m^{-3}) and only at depths below 50 m at RF and below 20 m at the ICE. The population at both stations was dominated by CV copepodites and adults. RF and ICE displayed the lowest abundances of *C. finmarchicus* ($\leq$187.3 ind m^{-3}, Fig. 5). Higher abundances of *C. finmarchicus* CI-CIII (117 ind m^{-3}) and *C. glacialis* CV (40 ind m^{-3}) and CIV (20 ind m^{-3}) were found between 0 to 20 m during the day than at night at RF, while *M. longa* adults were found in higher abundance (1.9 ind m^{-3}) towards the surface (20–50 m) at night at ICE.

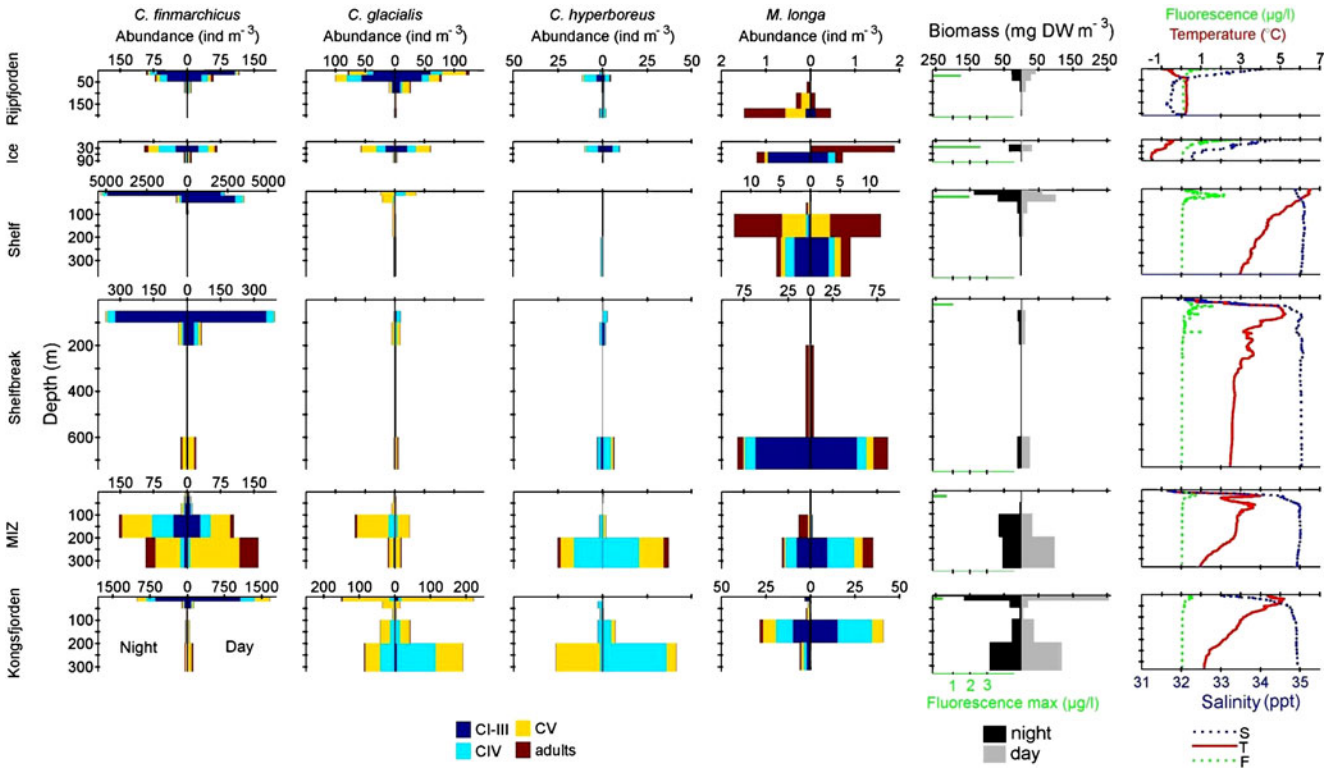

Fig. 5 Vertical profiles of *C. finmarchicus*, *C. glacialis*, *C. hyperboreus* and *M. longa* (individuals m^{-3}), *Calanus* biomass (mg DW m^{-3}), salinity, temperature (°C), and fluorescence (µg l^{-1}). Day samples are on the right axis of each plot, while night samples are on the left axis. The depth and intensity of the fluorescence maximum at each station is displayed on the biomass plots

At SH, *C. finmarchicus* dominated (>5,000 ind m^{-3}), and its population was composed almost entirely of CI-CIII copepodites. Higher abundances were found towards the surface (0–20 m) at night (4,920 ind m^{-3} at night compared with 2,076 ind m^{-3} during the day). Here, *C. hyperboreus* was rare, and a *C. glacialis* population dominated by CV copepodites was found between 0 to 50 m in comparatively low abundance (≤24 ind m^{-3}). *M. longa* was found in comparatively high numbers (>15 ind m^{-3}) and across all stages (CI–adult), and this *M. longa* population was found almost entirely below 100 m.

At the deeper SHB, a bimodal depth distribution was observed for all the copepod populations. *C. finmarchicus* dominated in higher abundances than at RF, ICE and MIZ (in excess of 500 ind m^{-3}). A younger population composed primarily of CI-CIII copepodites was found between 50 to 200 m (>90% of total 50–200 m abundance). In addition, an older population composed almost entirely of CV and adults was found at depths below 600 m. The *C. glacialis* and *C. hyperboreus* populations were found in low abundances at SHB (under 20 ind m^{-3}), but again displayed a bimodal depth distribution with the older stages at depth. *M. longa* was found in its highest abundances (in excess of 75 ind m^{-3}), and almost entirely below 600 m. This *M. longa* population was of mostly early stage animals, being composed >50% of CI-CIII copepodites.

At MIZ, *C. finmarchicus* and *C. hyperboreus* were more abundant than *C. glacialis* and *M. longa*, although abundances were similar to those at RF and ICE. The *C. finmarchicus* population at MIZ was dominated by the older copepodites (CV) and adults (>65% *C. finmarchicus* abundance), and was located primarily below 100 m. The *C. glacialis* population at MIZ was also dominated by CV (>90% *C. glacialis* abundance) and located below 100 m. More *C. finmarchicus* and *C. glacialis* individuals were found between 100 to 200 m during the night, and between 200 to 300 m during the day. The *C. hyperboreus* population here was composed more of CV copepodites and adults, and was located below 200 m. *M. longa* was found in high abundances (in excess of 70 ind m^{-3}) and predominantly below 200 m.

In KF, bimodal depth distributions (as at SHB) were observed among the copepods. Again, *C. finmarchicus* dominated in terms of abundance (up to 1,966 ind m^{-3}). The *C. finmarchicus* population above 50 m represented >90% of the total *C. finmarchicus* abundance, and was composed mainly of CI-CIII copepodites. The population at depth was older, and composed almost entirely of CV copepodites. In KF, *C. glacialis* was found

in its highest abundance (up to 473 ind m^{-3}). *C. glacialis* also displayed a bimodal depth distribution, but the two populations were similar in terms of abundance. The surface population (0–50 m depth) was composed almost entirely of CV copepodites, while the deeper population below 100 m was younger and composed of approximately 50% CIV copepodites alongside the CV stages. *C. hyperboreus* was also found here in comparatively high numbers, and almost entirely below 100 m. The *C. hyperboreus* stage composition was similar to *C. glacialis*, with CIV and CV dominating. *M. longa* had fairly high abundances in KF (in excess of 40 ind m^{-3}), and >70% of the population was located between 100 to 200 m; with considerably lower abundance (5.9 ind m^{-3}) at 200–300 m depth. The differences between day and night abundances were highest at KF, with considerably more copepods present in the day samples.

Vertical distribution of *Calanus* biomass

Converting the *Calanus* abundances to biomass (using a collection of published methods and species-specific mass-length relationships—see Zooplankton sampling) revealed considerably more biomass at shallow depths during the night than during the day at MIZ and SH (Fig. 5). In RF, more biomass was observed close to the surface during the day that at night. At MIZ, SHB and KF, most of the biomass was located below 200 m, while at RF, SH and ICE, most biomass was found in the upper 50 m.

Multivariate analysis of net samples

When the MPS determined abundances were compared between stations using a Bray-Curtis similarity matrix and one-way ANOSIM, significant differences were found between the depth stratified communities at each station (R=0.129, p=0.001), and between the depth strata at each station (R=0.224, p=0.001). SIMPER identified *C. finmarchicus* CI-CIII and *C. glacialis* CV as being most responsible for the differences in community between stations, while *C. finmarchicus* CI-CIII was most responsible for the differences between surface waters and deeper depths and *M. longa* CIII and CV were most responsible for the differences between 50 to 200 m and ≥200 m. Using these data, no significant difference was found between day and night samples (R=−0.022, p=0.829). Although the day and night samples are not significantly different to each other, SIMPER identified *C. finmarchicus* CI-CIII as being responsible for 25.31% of the differences between the day and night samples. Two-way ANOSIM analysis using station and time as the chosen factors resulted in no significant differences between stations (R=0.042, p=0.192) or day and night samples (R=−0.146, p=0.995).

Cluster analysis and ANOSIM of depth stratified total abundance showed significant differences between the stations (R=1, p=0.002), but high levels of similarity at all stations between the day and night samples taken at the same station (R=−0.164, p=0.952) (Fig. 6a). The highest similarities between day and night samples were found at ICE and SHB (>95% similar), and the lowest similarity at SH (<90% similar). When depth stratified total abundance was compared between stations, the ICE and RF were 75% similar, SHB and MIZ were >80% similar, and KF and SH were also >80% similar. SIMPER identified the 0–20 m depth strata as being most responsible (30%) for the differences between the day and night samples.

Cluster analysis and ANOSIM of the water column community diversity at each station again showed significant differences between the stations (R=1, p=0.002), but

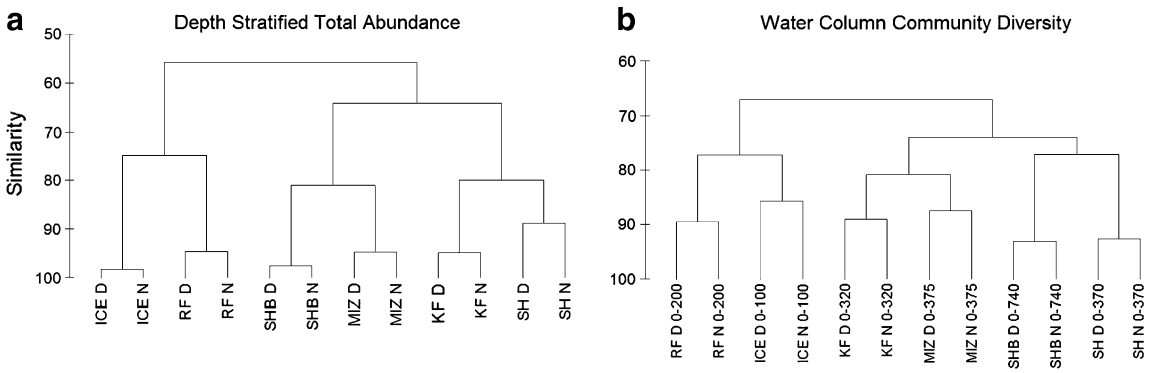

Fig. 6 Hierarchical cluster dendrograms based on Bray-Curtis similarity analysis on 4th-root transformed net abundance data. Similarity scale on cluster dendrograms represents percentage similarity between samples. *D* day sample, *N* night sample. **a** *Depth stratified total abundance* displays similarities between day and night samples at each station in terms of *Calanus* and *M. longa* abundance at each depth stratum. **b** *Water column community diversity* displays similarities between day and night samples at each station in terms of the abundance of every *Calanus* and *M. longa* stage integrated over the entire water column. The water column depths over which abundances are integrated is displayed on the dendrogram

less similarity between the day and night samples compared with the depth stratified total abundance (Fig. 6b). The difference, however, was very small (R=−0.154, p=0.922). The highest similarity between day and night samples was found at SH and SHB (>90% similar), and the lowest similarity at ICE (<90% similar).

200-kHz acoustics

Across all six stations, MVBS (S_v) was generally low (Fig. 7).

At RF, the 200-kHz data displayed low S_v values (−133 to −51 dB) throughout the upper 125 m during the day, with a scattering layer at approximately 0 to 85 m and a mean S_v of −80.68 dB. A scattering layer of higher mean S_v (−71.2 dB) was identified between 0 to 30 m during the night. When analysing the 200-kHz data (partitioned based on 120 kHz MVBS–38 kHz MVBS, Fig. 7), this surface scattering layer at night appeared to be primarily composed of mesozooplankton and macrozooplankton, but also contained some nekton echoes. At ICE, a similar pattern was observed but with higher S_v (−130 to −39 dB) and two backscattering layers: one between 0 to 80 m (−75 dB) during the day and 0 to 30 m (−68 dB) at night, the other near the bottom below 120 m (−88 dB) during the day and below 100 m (−81 dB) at night. Backscatter attributable to nekton was observed between 50 to 110 m during both the day and night, and appeared to be present mainly below the surface scattering layer. Mesozooplankton backscatter was found primarily in the two scattering layers during the day, and was more evenly spread throughout 0 to 125 m at night. Smaller mesozooplankton (ΔMVBS>20 dB) echoes were more prevalent within the surface scattering layer at night compared with the day. Echoes attributable to macrozooplankton (ΔMVBS of 2–12 dB) were found in both layers during the day and night, but at higher S_v (−79 to −77 dB) in the upper layer.

At SH, the echograms were characterised by the lowest S_v of any station. However, a generally diffuse distribution of backscatter during the day became more concentrated between 0 to 30 m at night. Though much of the backscatter deeper than 50 m during the day and night was attributed to mesozooplankton, the surface scattering layer appeared to be due to nekton during the day (Fig. 7), with more macrozooplankton and mesozooplankton backscatter towards the surface at night. At SHB, increased S_v below 100 m was observed at night (−87 to −76 dB at night compared with −99 to −81 dB during the day), and this was largely attributed to mesozooplankton. A patchy scattering layer was observed between 0 to 100 m during the day, and this scattering layer appears to be mostly due to macrozooplankton aggregations. Backscatter attributable to nekton was found between 0 to 125 m during both the day and night, but was most prevalent in a surface scattering layer between 0 to 50 m.

At MIZ, the day echogram was characterised by lower S_v (−89 to −78 dB) compared with the night echogram, with patches during the day being attributed more to macrozooplankton and mesozooplankton rather than nekton, and no clear scattering layer in the upper 125 m. However, S_v increased considerably at night in a similar manner to SHB, especially below 100 m (−81 to −72 dB) and in a surface scattering layer. On the basis of the two-frequency echo partition, this increase in backscatter below 100 m at night was largely attributed to mesozooplankton (Fig. 7). Echoes attributable to nekton were far more prevalent during the night than the day, especially between 0 to 75 m in a mixed scattering layer with macrozooplankton. At KF, a dense scattering layer of high S_v (−50 to −55 dB) was located below 100 m during the day. This backscatter was not attributed to fish alone (as the ΔMVBS is primarily >2 dB), and seemed to indicate a mixed layer of macrozooplankton and nekton. Amphipod backscatter should fall within this range, and the dense aggregation may have been composed of amphipods. A mesozooplankton scattering layer was also found at the same depth. However, at night, the dense high S_v scattering layer disappeared almost completely, and a scattering layer dominated by mesozooplankton remained. This layer was found below 50 m depth, with a higher ΔMVBS (>20 dB) indicating smaller mesozooplankton between 25 to 60 m and echoes mainly attributable to macrozooplankton between 0 to 20 m.

Multivariate analysis of acoustic measurements

When the partitioned 4th-root transformed 200-kHz acoustic backscatter (25-m×20-min grid, n=1,020) were compared between all sampled stations using a Bray-Curtis similarity matrix and one-way ANOSIM, significant differences were found between stations (R=0.15, p=0.001) but not between day and night samples (R=0.019, p=0.151). This difference between depth stratified stations is similar to the difference found using the net determined abundance data. However, when using a two-way ANOSIM with station and time as the chosen factors, significant differences were found between the depth stratified backscatter at each station (R=0.277, p=0.001), and also between the day and night samples (R=0.136, p=0.044). Significant differences were also found between the three classes of backscatter (mesozooplankton, macrozooplankton, nekton) at all stations using a one-way ANOSIM (R=0.055, p=0.018). The partitioned 200 kHz acoustic data are displayed as a MDS plot (Fig. 8a). Night mesozooplankton backscatter from RF, SH and KF along with night macrozooplankton backscatter from KF were

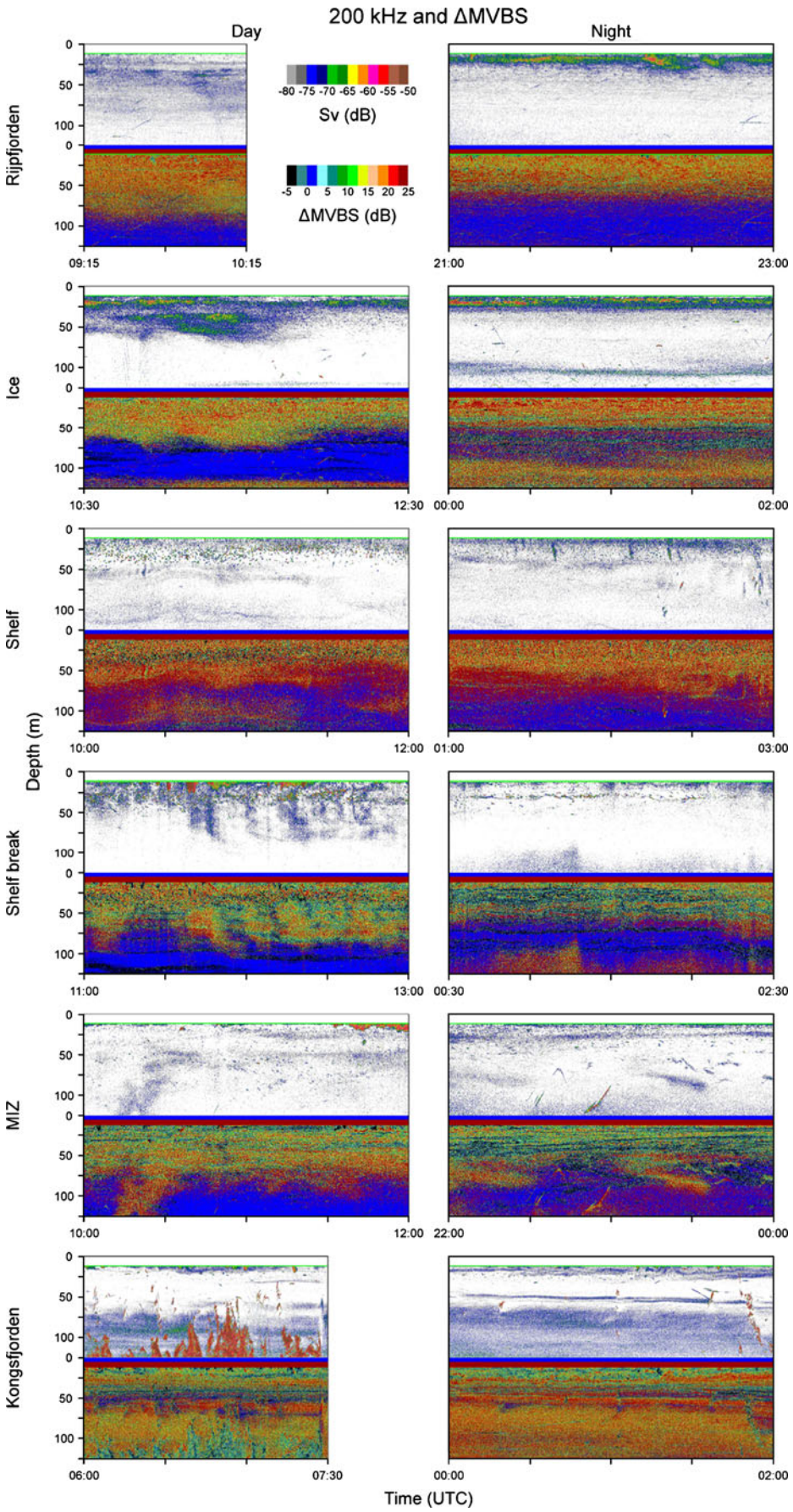

Fig. 7 The 200-kHz backscatter (*above*) and ΔMVBS (*below*) from each of the six stations (0–125 m depth). Volume backscatter (S_v) is expressed using a colour scale between −80 and −50 decibels (dB). ΔMVBS is expressed using a colour scale between −5 and 25 dB. The top 11 m of each echogram are discarded due to near-field and noise (i.e. *white* in the 200-kHz echogram and *dark blue/red solid stripe* on the ΔMVBS display). ΔMVBS echoes with *yellow-red shades* represent stronger scattering at 120 kHz, while ΔMVBS echoes with *grey-black shades* represent stronger scattering at 38 kHz. Day echograms are displayed on the *left* and night echograms on the *right*. UTC was 2 h behind local time during the study

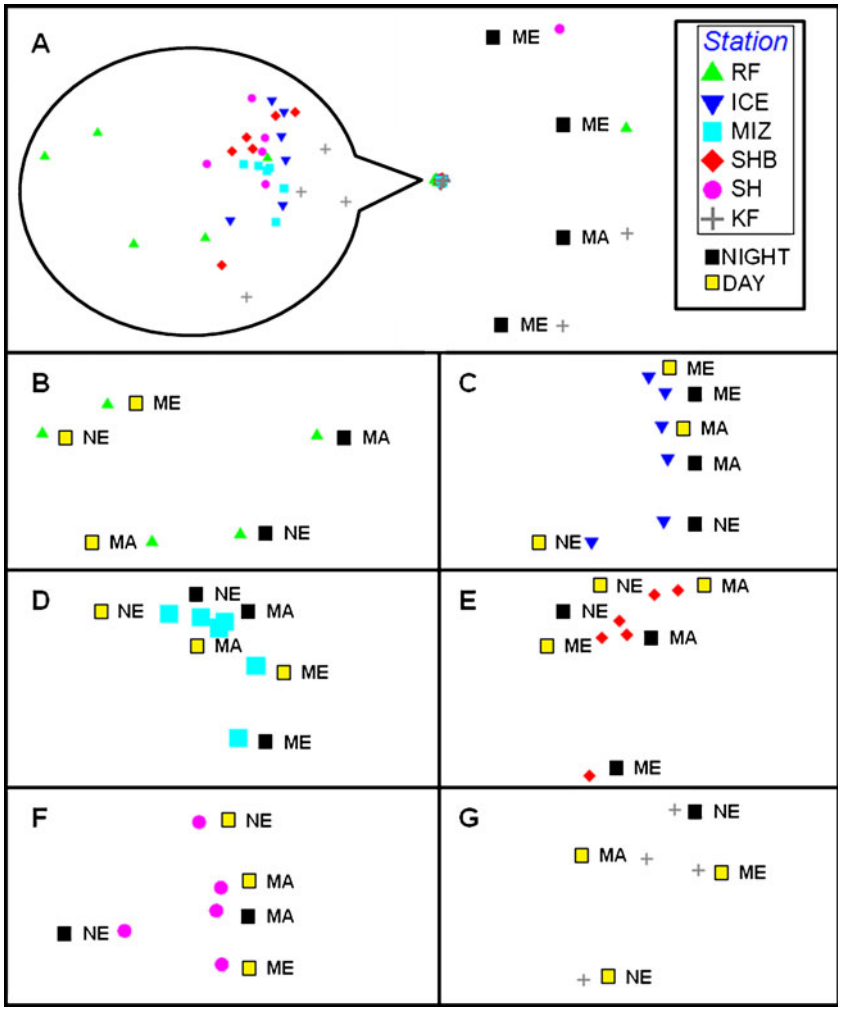

Fig. 8 **a** MDS plot based on Bray-Curtis similarity analysis on 4th-root transformed depth stratified acoustic data collected at 200 kHz at all stations (60-ping×1-m grid—0–125 m, n=1,020). Each station displays six points on the MDS plot—one each for mesozooplankton (ME), macroplankton (MA), and nekton (NE) during both the day (×3) and night (×3). Distances between points on the MDS represent similarity, with closer points being more similar. Stations and day/night symbols are indicated on the legend. *Inset* represents ×9 zoom on the close cluster in **a**. **b** (RF), **c** (ICE), **d** (MIZ), **e** (SHB), **f** (SH), and **g** (KF) are all expanded versions of **a** *inset* and display individual stations for clarity

the four outlying samples, with all other data being closely clustered. All six stations appeared to cluster with similar distances between samples, although RF (Fig. 8b) and KF (Fig. 8g) appeared to display the clearest and widest day/night separation.

When the three differently size groups were separated and analysed individually between stations, the resulting MDS plots (Fig. 9) confirmed RF and KF as most different in terms of their day and night acoustic data across all three classes of partitioned backscatter. RF and KF also displayed much greater distances between day and night backscatter at the macrozooplankton partition compared with the other stations (Fig. 9b), indicating that changes in macrozooplankton between day and night were of highest magnitude at these two stations. MIZ day and night data appeared to be most closely clustered and showed the least day/night differences of all stations. SH macrozooplankton (Fig. 9b) and nekton (Fig. 9c) day and night backscatter were relatively closely clustered, but the mesozooplankton (Fig. 9a) backscatter were not, indicating that mesozooplankton day/night differences were greater compared with the other stations and were therefore most important at SH. All p values were not significant during this analysis, although they indicated that day/night backscatter differences were largest for mesozooplankton and smallest for nekton.

ANOVA of acoustic measurements

When the partitioned 4th-root transformed 200-kHz acoustic backscatter (n=1,020) data were examined using a four-way ANOVA with station, taxa, time, and depth being the four tested factors, the only factor that exhibited significant influence was depth (F=2.7996, p=0.02496). However, when the other factors were ranked, time was the next most influential factor (F=2.5674, p=0.10940), followed by size (F=1.2213, p=0.29529) and station (F=1.0580, p=0.38223). In order to better resolve the differences between day and night measurements, depth was removed as an influencing factor by carrying out three-way ANOVA tests on individual depth strata (with station, taxa, and time now the only tested factors). These tests

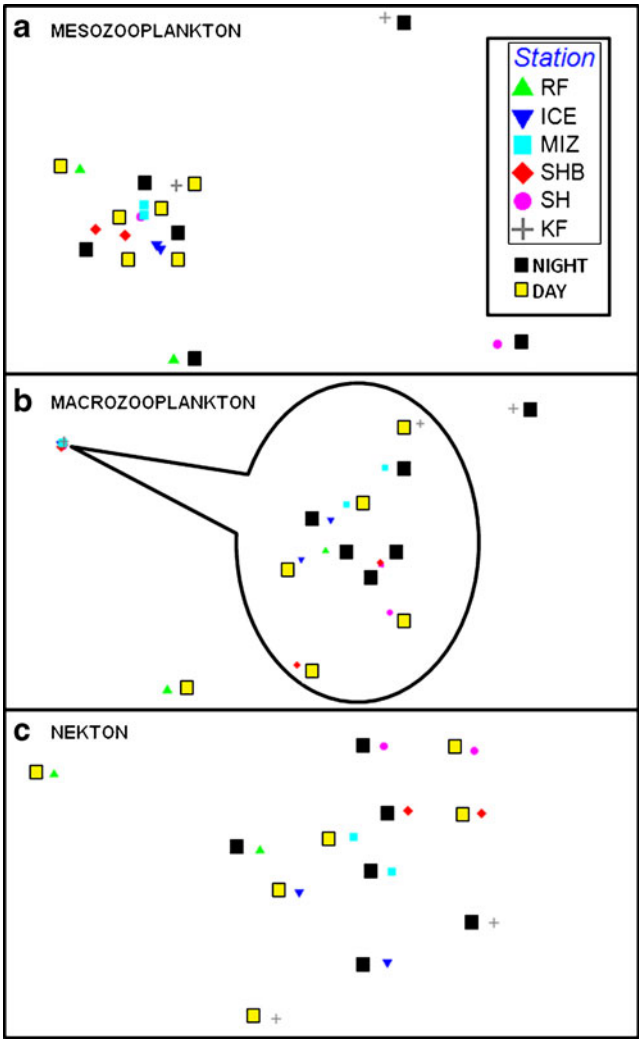

Fig. 9 MDS plots based on Bray-Curtis similarity analysis on 4th-root transformed depth stratified acoustic data collected at 200 kHz at all stations (60-ping×1-m grid—0–125 m, n=1,020). Acoustic data is split at each station based on ΔMVBS into (**a**) mesozooplankton, (**b**) macrozooplankton, and (**c**) nekton backscatter. Each station displays two points on each MDS plot—one for day and one for night backscatter. Distances between points on the MDS represent similarity, with closer points being more similar. *Inset* represents ×10 zoom on the close cluster in **b**. Stations and day/night symbols are indicated on the legend

highlighted station as a significant influencing factor at 25–50 m, 50–75 m, and 75–100 m ($4.2506<F<11.0649$, $2.149e^{-9}<p<0.001085$). The different taxa were never found to be a significant influencing factor on the differences in backscatter. However, time was a significant influencing factor at 25–50 m depth (F=6.1926, p=0.013666) and at 75–100 m depth (F=3.3836, p=0.06737). At 25–50 m, time was the strongest influencing factor on backscatter. Time was also the strongest influencing factor at 100–125 m, but the result was not significant (F=2.5918, p=0.1090)

Discussion

Seasonal 'snapshot'

The occurrence and timing of the High Arctic phytoplankton bloom is an important phenomenon (Zenkevitch 1963; Falk-Petersen et al. 2007; Søreide et al. 2008), and the bloom is shortest at higher latitudes. *Calanus* leave their over-wintering hibernations at depth and resume feeding at the surface in order to take advantage of the brief boom in high latitude primary production (Hagen 1999; Hagen and Auel 2001; Lee et al. 2006; Søreide et al. 2010), although the specific environmental signal that triggers the ascent from dormancy is unknown (Miller et al. 1991; Hirche 1996). This bloom period, which is habitually accompanied by higher intensities of light penetration in the water column, is associated with copepod DVM behaviour due to the trade-off between the need to feed at the surface and the need to escape visual predation by moving to depth. Although the six stations in our study were sampled at approximately the same time, they can be placed on a seasonal scale regarding their respective fluorescence maxima, and a clear seasonal pattern in the depth distribution and stage composition of the *Calanus* species can be observed.

ICE and RF can be considered "spring" stations in terms of their physical characteristics. At both of these stations, a noticeable fluorescence maximum was present at 25 to 30 m depth, corresponding to the boundary between surface MW and deeper AtW/ArW. Of all our sites, these stations were most recently dominated by ice cover (Fig. 2), and at RF in particular the ice cover had disappeared a day prior to sampling, which is consistent with the pronounced stratification and characterised an early bloom. Fluorescence data recorded by a mooring in Rijpfjorden indicated that the peak of the Arctic bloom had occurred very recently at this location (Wallace et al. 2010). Consequently, the *C. finmarchicus* and *C. glacialis* populations consisted predominantly of young stages concentrated in the upper 50 m, indicating that these stages were still actively feeding. Leu et al. (2010) described how the pelagic Arctic bloom in Rijpfjorden took place under the ice, just days/weeks before the ice break up, and that the first feeding stages of *C. glacialis* nauplii and copepodites were feeding actively on this phytoplankton bloom.

SH was influenced primarily by AtW and a pronounced fluorescence maximum existed there also (Fig. 5), indicating that bloom conditions prevailed at this location. As at RF and ICE, the mean depth of *C. finmarchicus* at SH was shallower than 50 m. However, *C. glacialis* and *C. hyperboreus* were concentrated below 100 m and up to 300 m depth at this location. The abundances of these species were very low at SH and SHB, as these areas were

outside their dominant areas of distribution (Daase and Eiane 2007; Blachowiak-Samolyk et al. 2008).

MIZ displayed a less pronounced fluorescence maximum, and a similarly low intensity fluorescence maximum was observed at SHB. The conditions at the two stations sampled in areas of broken sea-ice cover and large leads indicated either that the Arctic bloom had not yet occurred due to insufficient ice break up and light penetration into the water column, or that the annual season had progressed further at this location despite the relative closeness to the ice edge. The latter seems more likely due to the large leads present at the two stations. *C. finmarchicus* was concentrated considerably deeper here than at RF, ICE and SH (CI-CIII at 150 m and CIV-adults at 225 m) suggesting that the season had progressed far enough to prompt a descent to over-wintering depth. The *C. glacialis* and *C. hyperboreus* populations at MIZ and SHB followed a similar distribution that was deeper than their respective distributions at RF, ICE and SH. The pattern of seasonal vertical migration we observed, with copepods being found closer to the surface during the bloom and at depth (over-wintering) once the bloom had retreated with the ice edge (Wassmann et al. 2006) was in agreement with the widely documented seasonal regime in the High Arctic (Falk-Petersen et al. 2007, 2009; Varpe et al. 2007).

KF had a low fluorescence maximum at the time of sampling and, in terms of physical characteristics, can be considered the "furthest" from High Arctic spring conditions. Fluorescence data recorded by a mooring in KF confirmed that the peak of the spring bloom had occurred 2 to 3 months prior to sampling (Wallace et al. 2010).

At SHB and KF, a bimodal *Calanus* depth distribution was observed. *C. finmarchicus* CI-CIV were found primarily at the surface (0–75 m), while CV and adults dominated at depth (below 600 m at SHB and below 200 m at KF). This distribution indicates continued feeding at the surface from the younger copepodites, and a need to build lipid reserves even 2–3 months after the spring bloom. It is possible to infer that primary production and the food supply available to copepods was more plentiful at MIZ than at SHB and KF, as even the younger stages of *C. finmarchicus* at MIZ had retreated to depth, having presumably built up sufficient lipid reserves during the bloom. Furthermore, the respective depth distributions of copepods implied that the phytoplankton bloom was earlier at MIZ than at SHB, as more copepods are found over-wintering at depth. This inference is supported by the "seasonal" cluster dendrogram (Fig. 4), which places MIZ closer to KF and thus further from spring bloom conditions.

The "seasonal" separation of the sampling locations was reflected in the cluster dendrogram based on temperature, salinity and fluorescence data at each station (Fig. 4). However, dominant water mass characteristics at each station may have also played a key role in this clustering, with RF and ICE being heavily influenced by ArW (water temperature never exceeding 1°C), while all other stations appeared to be influenced by AtW (water temperatures of 4°C recorded). Heavy influence by AtW at KF is the primary factor keeping this fjord ice-free all year, thereby modifying the timing of the annual seasonal progression in the High Arctic.

Copepod DVM behaviour

Much of the debate surrounding the presence or absence of DVM amongst copepods revolves around both the seasonal variability and the mode of the behaviour. No conclusive evidence of synchronised DVM has been found using traditional depth stratified net sampling alone during the period of midnight sun (May) in the High Arctic (Blachowiak-Samolyk et al. 2006) and in early autumn (September) (Daase et al. 2008). However, substantial evidence of synchronised DVM during the autumn period (September) with a pronounced diel light cycle has been obtained using acoustic observation techniques alongside net sampling (Falk-Petersen et al. 2008). During the transitional period from summer to autumn, Cottier et al. (2006) determined that the period from July to September is the transitional period for a shift from unsynchronised vertical migration behaviour during midnight sun to a more classical synchronised DVM during autumn. However, that study used ADCP data primarily and was thus unable to identify the migrants involved. Our study falls within this transitional period, and a diel cycle was apparent at all stations in the PAR data. As our study was earlier in autumn than Falk-Petersen et al. (2008) (August 2–20 compared with September 2–9), we had the opportunity to study the transitional period at an earlier phase, and the broad spatial coverage of our six sampling locations allowed the comparison of sites with different phytoplankton bloom conditions during this period.

The MPS data indicated a classic DVM pattern at MIZ and SH, and reverse DVM signals in the abundances at RF (*C. finmarchicus and C. glacialis*) (Fig. 5) and ICE (*M. longa*). This apparent reverse DVM appeared to be strongest at RF, as suggested by the biomass distribution (Fig. 5). It is important to note that a combination of classic and reverse DVM will be difficult to detect amongst the acoustic backscatter, as the signals will effectively cancel one another out. Importantly, these observed differences in MPS abundance between the day and night samples were not statistically significant at any station, and the day and night samples were found to be very similar in terms of their total abundance at each depth stratum (Fig. 6a). SH day and night samples were most different from one another, and SIMPER analysis identified 0–20 m as being

the depth stratum most responsible (30%) for the difference. The greatest change in abundance between the day and night samples at this depth was by *C. finmarchicus*. These observations indicate that *C. finmarchicus* may be the dominant vertical migrator in and out of the surface 20 m.

The day and night samples from each station were less similar in terms of their community diversity at each station regardless of depth distribution (Fig. 6b), suggesting advective influences between day and night samples were stronger than vertical migration effects. However, the differences were very slight and not statistically significant. ICE day and night samples were most different from one another, suggesting that advection was more important at this location. Conversely, SH displayed the highest similarity between day and night community composition, but the lowest similarity in terms of copepod depth distribution, suggesting vertical migration was a stronger influence here.

Regardless of the day and night differences, copepod community depth distributions seemed to be grouped primarily by the dominant water masses influencing the stations (Fig. 6a). ICE and RF were 75% similar (ArW dominance); SHB and MIZ were >80% similar (transformed AtW dominance); and KF and SH were also >80% similar (AtW dominance). This result suggests that the different depth preferences between species that dominate in AtW (*C. finmarchicus*) and the species that dominate in ArW (*C. hyperboreus*) (Blachowiak-Samolyk et al. 2008) played a key role in copepod depth distribution.

Although "indications" of zooplankton DVM behaviour were gathered from the net-determined depth stratified abundances, no significant differences were found between the day and night samples ($-0.165<R<-0.022$). However, the 200 kHz acoustic measurements were made at higher vertical and temporal resolutions than the net samples, with 25–m depth resolution and six repeats every 20 min analysed. The 25-m depth resolution chosen ultimately provides better vertical resolution than the MPS system, and so is more effective at identifying smaller scale vertical signals. Multivariate analysis of these acoustic measurements resulted in significant differences between day and night backscatter across all stations, and using ANOVA allowed us to describe at which depths these day and night differences were significant. Although ANOVA described depth as being the strongest influencing factor on backscatter, time (day and night) was a significant influencing factor at 25–50 m and at 75–100 m.

KF and RF displayed the greatest differences between their day and night backscatter (Fig. 8). When these differences were compared with the advection versus vertical migration technique applied to the MPS samples (Fig. 6), it appeared that the differences could be in part due to advection. However, given that the largest contrasts between day and night MPS abundances were observed at KF (Fig. 5). It appears that this station is more likely than RF to be influenced by strong advection. This apparent advection signal is further complicated by the phenomenon of zooplankton distribution being very patchy in the marine ecosystem (Gallager et al. 1996). As the research vessel was drifting while on station, day and night MPS samples may have been taken in different "patches" of zooplankton. This sampling problem is partially addressed by using acoustic data collected continuously over a two hour period.

As the acoustic measurements were made at higher spatial and temporal resolutions than the MPS abundance data, the MPS data cannot be used effectively to inform the acoustic results. Unfortunately, only two MPS hauls (one day and one night) were available from each station. The day and night net hauls were also taken at different times of the day and night between stations (Table 1). This lack of directly comparable repeat data casts doubts over the results gathered from the MPS alone. However, these doubts can be addressed effectively by utilising the corroborating acoustic data, and this study illustrates how the two sampling methods can be used effectively in future studies, especially with repeated net sampling regimes. Furthermore, it is important to note that net samples are vital in identifying small acoustic targets and differentiating between vertical migrators.

Furthermore, acoustic targets outside the copepods studied here may be responsible for much of the acoustic DVM signal. These targets may be pteropods such as *Limacina helicina*, or pelagic amphipods such as *Themisto libellula* (Falk-Petersen et al. 2008) that are known to occur in high densities. At lower latitudes, pteropods are known to cause strong backscattering layers and to migrate vertically in diel cycles (Tarling et al. 2001), and these should be considered for future study. Notably, the MPS zooplankton net is not designed to catch fast swimming species like *T. libellula*. Our 200-kHz acoustic data contained backscatter contributions from both macrozooplankton and nekton (Fig. 7). The differences between day and night measurements of macrozooplankton in particular is strongest at RF and KF compared with the other stations, and this apparent macrozooplankton vertical migration could be largely responsible for the observed acoustic DVM signals at these two stations. However, multivariate analysis results showed that mesozooplankton backscatter had the greatest day/night differences overall across all the stations, making this taxa the most widespread vertical migrators across the study area.

Calanus populations feeding in near-surface waters appeared to undertake classic DVM to a greater extent

than *Calanus* populations that are no longer influenced by a pronounced fluorescence maximum. Both the acoustic and net data displayed a shallow water DVM signal at RF, ICE and SH, where a large portion of the population were still utilising the phytoplankton production at the surface. Thus, the copepods were located closer to the surface, and behaviour such as classic DVM that protects them from visual predation is a useful adaptation. *C. finmarchicus*, especially the younger stages (CI-CIII), appears to be most responsible for the differences between the sampled depths at all stations and also for the observed difference between the day and night samples (and *C. glacialis* CV to a lesser extent). This observation is in contrast to other studies that found the young developmental stages to be more stationary and confined to surface waters, while older stages displayed DVM behaviour (Tande 1988; Dale and Kaartvedt 2000; Daase et al. 2008). However, these observed differences among the younger stages of *C. finmarchicus* may not be good indications of a DVM signal, as advective effects and a lack of repeat MPS data influence any conclusion based solely on the net data. The observations may indicate instead that *C. finmarchicus* CI-CIII were subjected to the highest levels of advection, which is why their abundance was most different between day and night samples.

Conclusion

We conclude that zooplankton DVM occurs in the High Arctic during late summer/early autumn when changes in the diel light cycle are apparent, especially at 25 to 50 m depth. This low amplitude DVM is linked to the existence of a pronounced fluorescence maximum (approximately 30 m deep), and previous studies have shown that this tends to be most common during the Arctic bloom. Thus, we suggest that the occurrence of DVM should not be discussed in the context of annual timing and seasonal progression alone, but rather in the context of the High Arctic phytoplankton bloom that is potentially highly variable spatially, temporally, and in intensity. Our analyses indicate that advection is an important influence on zooplankton distributions, and has the potential to mask the signature of vertical migration. In addition to mesozooplankton DVM signals, macrozooplankton and nekton DVM can be important. Pronounced day/night differences in macrozooplankton vertical distribution were found at the fjord stations in particular, and as these predators may influence mesozooplankton behaviour, we consider a thorough understanding of the interactions between the different species of optimal importance. Such knowledge could be gained in future studies via a thorough and intensive net sampling regime.

Acknowledgements We would like to thank the Norwegian Polar Institute and the Scottish Association for Marine Science (especially Colin Griffiths, Finlo Cottier, Estelle Dumont and Ray Leakey) for their invaluable assistance with data collection and processing. Many thanks also to the scientists, officers and crew on board the RRS *James Clark Ross* for an effective sampling cruise. This publication was originally presented at the Arctic Frontiers Conference in Tromsø, January 2010. The support and initiative of ARCTOS and Arctic Frontiers are gratefully acknowledged. The study was funded in part by the Norwegian Research Council as part of the official IPY-project CLEOPATRA (project no. 178766/S60).

References

Arrigo KR, Thomas DN (2004) Large scale importance of sea-ice biology in the Southern Ocean. Antarct Sci 16:471–486

Basedow SL, Eiane K, Tverberg V, Spindler M (2004) Advection of zooplankton in an Arctic fjord (Kongsfjorden, Svalbard). Estuar Coast Shelf Sci 60:113–124

Benoit D, Simard Y, Fortier L (2008) Hydro-acoustic detection of large winter aggregations of Arctic cod (Boreogadus saida) at depth in ice-covered Franklin Bay (Beaufort Sea). J Geophys Res Oceans 113:C06S90. doi:10.1029/2007JC004276

Blachowiak-Samolyk K, Kwasniewski S, Richardson K, Dmoch K, Hop H, Falk-Petersen S, Mouritsen LT (2006) Arctic zooplankton do not perform diel vertical migration (DVM) during periods of midnight sun. Mar Ecol Prog Ser 308:101–116

Blachowiak-Samolyk K, Kwasniewski S, Hop H, Falk-Petersen S (2008) Magnitude of mesozooplankton variability: a case study from the Marginal Ice Zone of the Barents Sea in spring. J Plankton Res 30(3):311–323. doi:10.1093/plankt/fbn002

Cisewski B, Strass VH, Rhein M, Krägefsky S (2009) Seasonal variation of diel vertical migration of zooplankton from ADCP backscatter time series data in the Lazarev Sea, Antarctica. Deep-Sea Res (1 Oceanogr Res Pap). doi:10.1016/j.dsr.2009.10.005

Clarke KR, Gorley RN (2006) Primer v6: user manual/tutorial. Primer-E, Plymouth

Conover RJ, Huntley M (1991) Copepods in ice-covered seas - distribution, adaptations to seasonally limited food, metabolism, growth pattern and life cycle strategies in polar seas. J Mar Syst 2:l–41

Cottier FR, Tarling GA, Wold A, Falk-Petersen F (2006) Unsynchronised and synchronised vertical migration of zooplankton in a high arctic fjord. Limnol Oceanogr 51(6):2586–2599

Daase M, Eiane K (2007) Mesozooplankton distribution in northern Svalbard waters in relation to hydrography. Polar Biol 30 (8):969–981

Daase M, Vik JO, Bagøien E, Stenseth NC, Eiane K (2007) The influence of advection on *Calanus* near Svalbard: statistical relations between salinity, temperature and copepod abundance. J Plankton Res 29(10):903–911. doi:10.1093/plankt/fbm068

Daase M, Eiane K, Aksnes DL, Vogedes D (2008) Vertical distribution of *Calanus* spp. and *Metridia longa* at four Arctic locations. Mar Biol Res 4:193–207

Dale T, Kaartvedt S (2000) Diel patterns in stage-specific vertical migration of *Calanus finmarchicus* in habitats with midnight sun. ICES J Mar Sci 57:1800–1818

Falkenhaug T, Tande KS, Semenova T (1997) Diel, seasonal and ontogenetic variations in the vertical distributions of four marine copepods. Mar Ecol Prog Ser 149:105–119

Falk-Petersen S, Hopkins CCE, Sargent JR (1990) Trophic relationships in the pelagic arctic food web. In: Barnes M, Gibson RN (eds) Trophic relationships in the marine environment. Aberdeen Univ Press, Aberdeen, pp 315–333

Falk-Petersen S, Pedersen G, Kwasniewski S, Hegseth EN, Hop H (1999) Spatial distribution and life-cycle timing of zooplankton in the marginal ice zone of the Barents Sea during the summer melt season in 1995. J Plankton Res 21:1249–1264

Falk-Petersen S, Hagen W, Kattner G, Clarke A, Sargent J (2000) Lipids, trophic relationships, and biodiversity in Arctic and Antarctic krill. Can J Fish Aquat Sci 57(S3):178–191

Falk-Petersen S, Timofeev S, Pavlov V, Sargent JR (2007) Climate variability and possible effects on Arctic food chains: the role of Calanus. In: Ørbæk JB, Tombre T, Kallenborn R, Hegseth E, Falk-Petersen S, Hoel AH (eds) Arctic alpine ecosystems and people in a changing environment. Springer, Berlin

Falk-Petersen S, Leu E, Berge J, Kwasniewski S, Nygard H, Rostad A, Keskinen E, Thormar J, von Quillfeldt C, Wold A, Gulliksen B (2008) Vertical migration in high Arctic waters during autumn 2004. Deep–Sea Res (2 Top Stud Oceanogr). doi:10.1016/j.dsr2.2008.05.010

Falk-Petersen S, Mayzaud P, Kattner G (2009) Lipids, life strategy and trophic relationships of *Calanus hyperboreus*, *C. glacialis* and *C. finmarchicus* in the Arctic. Mar Biol Res 5(1):18–39

Fischer J, Visbeck M (1993) Seasonal variation of the daily zooplankton migration in the Greenland Sea. Deep–Sea Res (1 Oceanogr Res Pap) 40:1547–1557

Gallager SM, Davis CS, Epstein AW, Solow A, Beardsley RC (1996) High-resolution observations of plankton spatial distributions correlated with hydrography in the Great South Channel, Georges Bank. Deep–Sea Res (2 Top Stud Oceanogr) 43(7–8):1627–1663

Gosselin M, Levasseur M, Wheeler PA, Horner RA, Booth BC (1997) New measurement of phytoplankton and ice algal production in the Arctic Ocean. Deep–Sea Res (2 Top Stud Oceanogr) 44 (8):1623–1644

Hagen W (1999) Reproductive strategies and energetic adaptations of polar zooplankton. Invertebr Reprod Dev 36(1–3):25–34

Hagen W, Auel H (2001) Seasonal adaptations and the role of lipids in oceanic zooplankton. Zool-Anal Complex Sy 104(3–4):313–326

Hays GC (2003) A review of the adaptive significance and ecosystem consequences of zooplankton diel vertical migrations. Hydrobiologia 503:163–170

Heath MR, Boyle PR, Gislason A, Gurney WSC, Hay SJ, Head EJH, Holmes S et al (2004) Comparative ecology of over-wintering *Calanus finmarchicus* in the northern North Atlantic, and implications for life-cycle patterns. ICES J Mar Sci 61:698–708

Hegseth EN, Sundfjord A (2008) Intrusion and blooming of Atlantic phytoplankton species in the High Arctic. J Mar Syst 74(1–2):108–119

Hirche H-J (1991) Distribution of dominant calanoid copepod species in the Greenland sea during late fall. Polar Biol 11(6):351–362

Hirche H-J (1996) Diapause in the marine copepod *Calanus finmarchicus*—a review. Ophelia 44:129–143

Hirche H-J (1997) Life cycle of the copepod *Calanus hyperboreus* in the Greenland Sea. Mar Biol 128:607–618

Hunt GL Jr, Stabeno P, Walters G, Sinclair E, Brodeur RD, Napp JM, Bond NA (2002) Climate change and control of the southeastern Bering Sea pelagic ecosystem. Deep–Sea Res (2 Top Stud Oceanogr) 49:5821–5853

Karnovsky NJ, Weslawski JM, Kwasniewski S, Walkusz W, Beszczynska-Moeller A (2003) The foraging behaviour of Little Auks in a heterogeneous environment. Mar Ecol Prog Ser 253:289–303

Kosobokova KN (1978) Diurnal vertical distribution of *Calanus hyperboreus* Kroyer and *Calanus glacialis* Jaschnov in the Central Polar Basin. Oceanology 18:476–480

Kwasniewski S, Hop H, Falk-Petersen S, Pedersen G (2003) Distribution of *Calanus* species in Kongsfjorden, a glacial fjord in Svalbard. J Plankton Res 25(1):1–20

Lee RF, Hagen W, Kattner G (2006) Lipid storage in marine zooplankton. Mar Ecol Prog Ser 307:273–306

Leu E, Falk-Petersen S, Kwasniewski S, Wulff A, Edvardsen K, Hessen DO (2006) Fatty acid dynamics during the spring bloom in a High Arctic fjord: importance of Abiotic factors versus community changes. Can J Fish Aquat Sci 63 (12):2760–2779

Leu E, Søreide JE, Hessen DO, Falk-Petersen S, Berge J (2010) Consequences of changing sea-ice cover for primary and secondary producers in the Arctic: timing, quantity and quality. Prog Oceanogr (in press)

Longhurst AR (1976) Interactions between zooplankton and phytoplankton profiles in the eastern tropical Pacific Ocean. Deep-Sea Res 23:729–754

Longhurst AR, Williams R (1992) Carbon flux by seasonal vertical migrant copepods is a small number. J Plankton Res 14:1495–1509

Longhurst AR, Sameoto D, Herman A (1984) Vertical distribution of Arctic zooplankton in summer: eastern Canadian archipelago. J Plankton Res 6(1):137–168

Longhurst AR, Bedo AW, Harrison WG, Head EJH, Sameoto DD (1990) Vertical flux of respiratory carbon by oceanic diel migrant biota. Deep-Sea Res 37:685–694

Madureira LSP, Everson I, Murphy EJ (1993) Interpretation of acoustic data at two frequencies to discriminate between Antarctic krill (*Euphausia superba* Dana) and other scatterers. J Plankton Res 15(7):787–802

Miller CB, Cowles TJ, Wiebe PH, Copley NJ, Grigg H (1991) Phenology in *Calanus finmarchicus*; hypotheses about control mechanisms. Mar Ecol Prog Ser 72:97–91

Mumm N (1991) On the summerly distribution of mesozooplankton in the Nansen Basin, Arctic Ocean (in German). Rep Polar Res 92:1–173

Piechura J, Beszczynska-Moeller A, Osinski R (2001) Volume, heat and salt transport by the West Spitsbergen Current. Polar Res 20:233–240

Richter C (1994) Regional and seasonal variability in the vertical distribution of mesozooplankton in the Greenland Sea. Rep Polar Res 154:1–87

Sakshaug E, Slagstad D (1991) Light and productivity of phytoplankton in marine ecosystems: a physiological view. Polar Res 10:69–85

Sampei M, Sasaki H, Hattori H, Fukuchi M, Hargrave BT (2004) Fate of sinking particles, especially faecal pellets, within the epipelagic zone in the North Water (NOW) polynya of northern Baffin Bay. Mar Ecol Prog Ser 278:17–25

Smetacek V, Nicol S (2005) Review polar ocean ecosystems in a changing world. Nature 437:362–368

Smith WO, Sakshaug E (1990) Autotrophic processes in polar regions. In: Smith WO (ed) Polar oceanography. Part B. Academic Press, San Diego, pp 477–525

Søreide JE, Hop H, Carroll ML, Falk-Petersen S, Hegseth EN (2006) Seasonal food web structures and sympagic-pelagic coupling in the European Arctic revealed by stable isotopes and a two-source food web model. Prog Oceanogr 71(1):59–87

Søreide JE, Falk-Petersen S, Hegseth EN, Hop H, Carroll ML, Hobson KA, Blachowiak-Samolyk K (2008) Seasonal feeding strategies of *Calanus* in the high-Arctic Svalbard region. Deep–Sea Res (2 Top Stud Oceanogr). doi:10.1016/j.dsr2.2008.05.024

Søreide JE, Leu E, Berge J, Graeve M, Falk-Petersen S (2010) Effects of omega-3 fatty acid production on *Calanus glacialis* reproduction and growth in a changing marine Arctic. Glob Change Biol. doi:10.1111/j.1365-2486.2010.02175.x

Svendsen H et al (2002) The physical environment of Kongsfjorden-Krossfjorden, an Arctic fjord system in Svalbard. Polar Res 21 (1):133–166

Tande K (1988) An evaluation of factors affecting vertical distribution among recruits of *Calanus finmarchicus* in three adjacent high latitude localities. Hydrobiologia 167:115–126

Tarling GA, Matthews JBL, David P, Guerin O, Buchholz F (2001) The swarm dynamics of northern krill (*Meganyctiphanes norvegica*) and pteropods (*Cavolinia inflexa*) during vertical migration in the Ligurian Sea observed by an acoustic Doppler current profiler. Deep-Sea Res (1 Oceanogr Res Pap) 48 (7):1671–1686

Unstad KH, Tande K (1991) Depth distribution of *Calanus finmarchicus* and *C. glacialis* in relation to environmental conditions in the Barents Sea. Polar Res 10:409–420

Varpe Ø, Jørgensen C, Tarling GA, Fiksen Ø (2007) Early is better: seasonal egg fitness and timing of reproduction in a zooplankton life-history perspective. Oikos 116:1331–1342. doi:10.1111/j.2007.0030-1299.15893.x

Vinogradov ME (1997) Some problems of vertical distribution of meso- and macroplankton in the ocean. Adv Mar Biol 32:1–92

Walkusz W, Storemark K et al (2003) Zooplankton community structure; a comparison of fjords, open water and ice stations in the Svalbard area. Pol Polar Res 24(2):149–165

Wallace MI, Cottier FR, Berge J, Tarling GA, Griffiths C, Brierley AS (2010) Comparison of zooplankton vertical migration in an ice-free and a seasonally ice-covered Arctic fjord: an insight into the influence of sea-ice cover on zooplankton behaviour. Limnol Oceanogr 55(2):831–845

Wassmann P, Reigstad M, Haug T, Rudels B, Carroll ML, Hop H, Gabrielsen GW, Falk-Petersen S, Denisenko SG, Arashkevich E, Slagstad D, Pavlova O (2006) Food webs and carbon flux in the Barents Sea. Prog Oceanogr 71(2–4):232–287

Watkins JL, Brierley AS (1996) A post-processing technique to remove background noise from echo integration data. ICES J Mar Sci 53:339–344

Wexels RC, Wassmann P, Olli K, Pasternak A, Arashkevich E (2002) Seasonal variation in production, retention and export of zooplankton faecal pellets in the marginal ice zone and the central Barents Sea. J Mar Syst 38:175–188

Willis KJ, Cottier FR, Kwasniewski S, Wold A, Falk-Petersen S (2006) The influence of advection on zooplankton community composition in an Arctic fjord (Kongsfjorden, Svalbard). J Mar Syst 61:39–54. doi:10.1016/j.jmarsys.2005.11.013

Yoshida T, Toda T, Kuwahara V, Taguchi S, Othman BHR (2004) Rapid response to changing light environments of the calanoid copepod *Calanus sinicus*. Mar Biol 145(3):505–513

Zenkevitch L (1963) Biology of the seas of the USSR. George Allen and Unwin, London